positive oxidation state of manganese and makes it a poor oxidizing agent.[24] The participation of the phosphate ligand is also reflected in the molar absorptivity of the intermediate at 505 nm (Table III). (iv) The molar absorptivities calculated (in the absence of pyrophosphate) at various wavelengths (Table III) point to an absorption band near 500 nm, in common with other (amino polycarboxylato)manganese(III) complexes.[25] (v) The molar absorptivity of this species, 300 M^{-1} cm^{-1} at 505 nm lies between the values observed for Mn^{III}(HEDTA) (HEDTA = hydroxyethylethylenediaminetriacetic acid) and Mn^{III}(EDTA), as expected if the partially oxidized EDTA is coordinated to this metal center. (vi) The rate constant for the decomposition of the intermediate is close to the values observed for the decomposition of other Mn(III)–amino polycarboxylato complexes[25,26] as discussed below.

The formation of EDTA oxidized products may proceed through several steps such as decarboxylation and subsequent formation of alcohol and aldehyde and finally a second decarboxylation reaction. Suggested routes that would lead to EDTRI and CO_2 are depicted in Scheme I.[27] A $4e^-$ oxidation product, an aldehyde (III), may coexist with the Mn(III) intermediate if the subsequent reaction of this organic product with MnO_4^- proceeds more slowly than the corresponding reaction with the Mn(III) intermediate. Second-order rate constants for oxidations of aliphatic aldehydes[28] with MnO_4^- have been reported to lie in the range 2–5 M^{-1} s^{-1} corresponding to a first-order rate constant, (4–10) × 10^{-4} s^{-1}, considering that 20% of the Mn exists as intermediate at its peak concentration.

Since the molar absorptivity of the intermediate is less than that of Mn^{III}(EDTA) at its absorption maximum, a partially oxidized EDTA molecule, perhaps an aldehyde (III) (a $4e^-$ oxidation product) may be coordinated to the Mn(III) center. In the presence of pyrophosphate ion, the intermediate is more probably a mixed-ligand complex in which pyrophosphate and partially oxidized EDTA are attached to the manganese center. Hamm and co-workers[24,25] reported that Mn^{III}(HEDTA) decomposes about seven times faster (4.2 × 10^{-5} s^{-1}) than Mn^{III}(EDTA) (for which Mn^{III}(EDTRI), CO_2, and H_2CO were identified as products). The intermediate in this study decomposes seven times faster than these amino polycarboxylato complexes of Mn(III). The first-order decomposition of the intermediate is proposed to be an internal electron transfer[29] to form Mn(II) and organic oxidation products, as shown in Scheme I.

Acknowledgment. Support of this research by the Kent State University Research Council is gratefully acknowledged. We are indebted to Professor E. S. Gould for incisive comments on this work and for carefully reading the manuscript.

(23) A retardation in decomposition of the intermediate by pyrophosphate ion may not alone be sufficient to justify a Mn(III) intermediate. The same ligand may also be a scavenger for Mn(IV). Freeman and co-workers[21] argued that some of the reported Mn(III) intermediates[16] in organic oxidations by permanganate ions should be Mn(IV) species, instead. Our other data (see text) are more consistent for a Mn(III) than a Mn(IV) intermediate.

(24) Watters, J. I.; Kolthoff, I. M. *J. Am. Chem. Soc.* **1948**, *70*, 2455. Davies, G. *Coord. Chem. Rev.* **1969**, *4*, 199.

(25) Hamm, R. E.; Suwyn, M. A. *Inorg. Chem.* **1967**, *6*, 139. Diebler, H.; Sutin, N. *J. Phys. Chem.* **1964**, *68*, 174. Davis, T. S.; Fackler, J. P.; Neeks, M. J. *Inorg. Chem.* **1968**, *7*, 1994.

(26) Schroeder, K. A.; Hamm, R. E. *Inorg. Chem.* **1964**, *3*, 391.

(27) The proposed scheme does not rule out sequential 1e transfer processes that might generate various species during the reaction. The scheme elucidates various pathways by which the final products (EDTRI and CO_2) are formed with the number of electrons involved in each step.

(28) Freeman, F.; Lin, D. K.; Moore, G. R. *J. Org. Chem.* **1982**, *47*, 56.

(29) An alternative in which a second EDTA molecule forms a complex with the intermediate, followed by an internal electron-transfer step (k_{et}), would be mechanistically indistinguishable if the formation constant (K) were >500 M^{-1}:

$$(\text{P-EDTA})Mn^{III} + \text{EDTA} \overset{K}{\rightleftharpoons} (\text{P-EDTA})Mn^{III}\text{–EDTA}$$

$$(\text{"P-EDTA"})Mn^{III}(\text{EDTA}) \xrightarrow{k_{et}} Mn(II) + \text{EDTRI} + CO_2 + \text{EDTA}$$

"P-EDTA" is the partially oxidized EDTA molecule attached to Mn(III), as discussed in the text.

Contribution from the Kenan Laboratories of Chemistry, The University of North Carolina, Chapel Hill, North Carolina 27599-3290

Cryoelectrochemical Study of the Cleavage of Radical Anions of Diiron and Diruthenium Carbonyl Dimers

E. F. Dalton,† Stanton Ching,‡ and Royce W. Murray*

Received December 20, 1990

Electrochemical reduction of the diiron complexes $[Fe(CO)_2(\eta^5\text{-Cp})]_2$ and $[Fe(CO)_2(\eta^5\text{-Cp}^*)]_2$ proceeds at room temperature by two electrons, but at low temperature is a one-electron reaction producing dimer radical anions that are stable on the voltammetric time scale. Analysis of the reaction kinetics at intervening temperatures shows that the two-electron reaction occurs through the radical anion, which dissociates to a mononuclear anion and a radical. The second electron is delivered homogeneously to the radical by a second dimer radical anion. The cleavage rate constant for $[Fe(CO)_2(\eta^5\text{-Cp})]_2^{\bullet-}$ is 10^2 times that for $[Fe(CO)_2(\eta^5\text{-Cp}^*)]_2^{\bullet-}$ (at 0 °C), and the rate for the related dimer $[Ru(CO)_2(\eta^5\text{-Cp})]_2^{\bullet-}$ was too fast to measure and at least 10^4 times larger than that for $[Fe(CO)_2(\eta^5\text{-Cp}^*)]_2^{\bullet-}$. The rates of the dimer radical anion cleavage fall in the same order as the rates of isomer interconversion in the parent dimers and raise the possibility that the rate of cleavage may be controlled by an intramolecular cleavage-precursor step.

The photochemical[1-6] and electrochemical[7-16] reactivity of fluxional, carbonyl-bridged metal dimers like those in Figure 1 has been an active area of research. Their reactions yield a variety of products, including mononuclear anions of the form $[M(CO)_2(\eta^5\text{-Cp})]^-$, which can be prepared by both electrochemical[12-16] and chemical reductive cleavage.[17,18] While the electrochemically induced dimer cleavage was first[13,14] described to occur via a two-electron-reduced dimer, Parker and co-workers[12] later reported that electrochemical cleavage of $[Fe(CO)_2(\eta^5\text{-Cp})]_2$ (1) occurs following one-electron reduction to the dimer radical anion.

† Present address: Grove City College, Grove City, PA 16127.
‡ Present address: Connecticut College, New London, CT 06320.

(1) Meyer, T. J.; Casper, J. V. *Chem. Rev.* **1985**, *85*, 187.
(2) Meyer, T. J. *Prog. Inorg. Chem.* **1975**, *19*, 1.
(3) Wrighton, M. S. *Chem. Rev.* **1974**, *74*, 401.
(4) Casper, J. V.; Meyer, T. J. *J. Am. Chem. Soc.* **1980**, *102*, 7794.
(5) Abrahamson, H. B.; Palazzotto, M. C.; Reichel, C. L.; Wrighton, M. S. *J. Am. Chem. Soc.* **1979**, *101*, 4123.
(6) Hepp, A. F.; Biaha, J. P.; Lewis, C.; Wrighton, M. S. *Organometallics* **1984**, *3*, 174.
(7) Bullock, J. P.; Palazotto, M. C.; Mann, K. R. Personal communication, 1990.
(8) Ferguson, J. A.; Meyer, T. J. *Inorg. Chem.* **1971**, *10*, 1025.

0020-1669/91/1330-2642$02.50/0

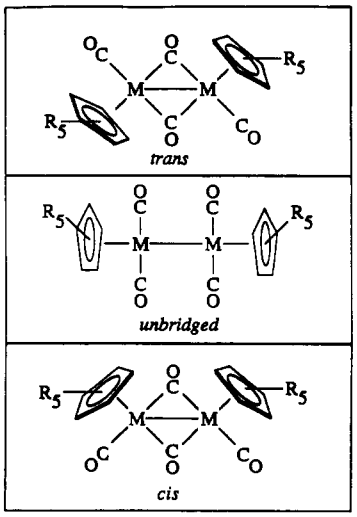

Figure 1. Metal dimer systems investigated and their isomeric forms. $[Fe(CO)_2(\eta^5\text{-Cp})]_2$ exists as a cis isomer and to a small extent in unbridged form, $[Fe(CO)_2(\eta^5\text{-Cp*})]_2$ exists only as the trans isomer, and $[Ru(CO)_2(\eta^5\text{-Cp})]_2$ exists in significant amounts in all three forms.

This paper presents a further cryoelectrochemical study of electroreductive cleavage of the $[Fe(CO)_2(\eta^5\text{-Cp})]_2$ dimer and also of the related permethyl-substituted derivative $[Fe(CO)_2(\eta^5\text{-Cp*})]_2$ and the ruthenium analogue $[Ru(CO)_2(\eta^5\text{-Cp})]_2$. We confirm the results of Parker and co-workers[12] and at reduced temperatures are able to observe and measure the cleavage kinetics of the one-electron diiron intermediates. The reduced ruthenium dimer is too unstable to observe a one-electron intermediate even at −76 °C. The cleavage rate constants vary by at least 10^5-fold among the three dimer radical anions.

The three isomeric dimer forms are depicted in Figure 1 and are known to differ substantially with respect to the preferred isomer and the rates of isomeric interconversion.[5,19-21] In polar solvents, $[Ru(CO)_2(\eta^5\text{-Cp})]_2$ exists[5] in appreciable amounts in bridged and unbridged forms with the equilibrium shifting toward the bridged form at lowered temperature. In contrast, $[Fe(CO)_2(\eta^5\text{-Cp})]_2$ predominantly exists in bridged forms (with more[6,21] cis than trans), while $[Fe(CO)_2(\eta^5\text{-Cp*})]_2$ exists only as the bridged, trans form in solution.[5] $[Ru(CO)_2(\eta^5\text{-Cp})]_2$ undergoes much more rapid terminal/bridging CO interconversion[19-21] than does $[Fe(CO)_2(\eta^5\text{-Cp})]_2$. We will consider the possible relationship between these isomeric properties and the electrochemical cleavage kinetics.

Room-temperature electrolysis of metal dimer ($[M(CO)_2(\eta^5\text{-Cp})]_2$) solutions has demonstrated[13-15] that two electrons are consumed at the potential of the dimer reduction wave, producing a mononuclear anion:

$$[M(CO)_2(\eta^5\text{-Cp})]_2 + 2e^- \rightleftarrows 2[M(CO)_2(\eta^5\text{-Cp})]^- \quad (1)$$

The first of two possible mechanistic pathways for this process is the delivery of two electrons to the dimer followed by homolytic cleavage of its dianion, $[M(CO)_2(\eta^5\text{-Cp})]_2^{2-}$, in an "$E_rC_i$" mechanism, where k_{obs} is a first-order rate constant:

$$[M(CO)_2(\eta^5\text{-Cp})]_2 + 2e^- \rightleftarrows [M(CO)_2(\eta^5\text{-Cp})]_2^{2-} \quad (2)$$

$$[M(CO)_2(\eta^5\text{-Cp})]_2^{2-} \xrightarrow{k_{obs}} 2[M(CO)_2(\eta^5\text{-Cp})]^- \quad (3)$$

The second pathway involves delivery of one electron followed by heterolytic cleavage of the dimer radical anion, where following its first-order (k_1) production, the radical fragment $[M(CO)_2(\eta^5\text{-Cp})]^\bullet$ is reduced either at the electrode surface or in a homogeneous manner in a second-order step (k_2) by $[M(CO)_2(\eta^5\text{-Cp})]_2^{\bullet-}$:

$$[M(CO)_2(\eta^5\text{-Cp})]_2 + e^- \rightleftarrows [M(CO)_2(\eta^5\text{-Cp})]_2^{\bullet-} \quad (4)$$

$$[M(CO)_2(\eta^5\text{-Cp})]_2^{\bullet-} \xrightarrow{k_1} [M(CO)_2(\eta^5\text{-Cp})]^- + [M(CO)_2(\eta^5\text{-Cp})]^\bullet \quad (5)$$

$$[M(CO)_2(\eta^5\text{-Cp})]^\bullet + e^- \rightleftarrows [M(CO)_2(\eta^5\text{-Cp})]^- \quad (6)$$

$$[M(CO)_2(\eta^5\text{-Cp})]^\bullet + [M(CO)_2(\eta^5\text{-Cp})]_2^{\bullet-} \xrightarrow{k_1} [M(CO)_2(\eta^5\text{-Cp})]_2 + [M(CO)_2(\eta^5\text{-Cp})]^- \quad (7)$$

The extent to which reaction 6 contributes depends on the relative values of k_1 and k_2. If the cleavage of $[M(CO)_2(\eta^5\text{-Cp})]_2^{\bullet-}$ is the slower step, the reaction kinetics will be first order.

Our observations show that the behavior of the two iron dimers, observed by using double potential step chronoamperometry (DPSCA) and rotated ring–disk voltammetry (RRDE), is consistent with the second of the above pathways with rate control by reaction 5 or by an intramolecular precursor to reaction 5.

Experimental Section

Chemicals. Bis(cyclopentadienyldicarbonyliron) dimer (Fluka), bis((pentamethylcyclopentadienyl)dicarbonyliron) dimer (Strem), and bis(cyclopentadienyldicarbonylruthenium) dimer (Strem) were used as recieved. Tetrabutylammonium hexafluorophosphate (Bu_4NPF_6, Fluka) was dried in a vacuum oven (50 °C) for at least 2 days, propionitrile and tetrahydrofuran (THF) were vacuum-distilled, and butyronitrile was distilled from CaH_2 under N_2, prior to use. Standard vacuum-line and syringe techniques were used to transfer solvents.[23]

Equipment. Standard three- and four-electrode configurations were used with a Pine Instruments Model ARDE-4 bipotentiostat and Model AFMSRX electrode rotator. A PAR Model 175 voltage source generated square and triangle wave sequences for double potential step chronoamperometry and cyclic voltammetry, which were recorded with a Nicolet Model 2040 digital oscilloscope and transferred to a microcomputer for analysis. The potential of the silver wire pseudoreference electrode was stable over the duration of a given experiment and was occasionally checked vs the ferrocene(0/1+) couple. The kinetic measurements do not depend on knowing precise electrode potentials. Potentials are reported vs SCE. Electrochemical cells were cooled in slush baths, whose literature[24] temperatures were verified (±1 °C) by using copper–constantan thermocouples (Omega).

Rotated Ring–Disk Electrode (RRDE) Voltammetry. The RRDE cell was a 100-mL Kjeldahl flask equipped with a 4-mm Teflon/glass side-arm valve (screw type) and a 25-mm O-ring joint at the mouth of the flask. Samples of $[Fe(CO)_2(\eta^5\text{-Cp})]_2$ and electrolyte were introduced; the flask was purged with N_2, and 50 mL of dry, deaerated solvent was added by syringe. Next, the cap was removed under nitrogen purge and replaced with a rubber O-ring to which were attached (with Torr-Seal) wires leading to Pt-mesh auxiliary and Ag-wire reference electrodes positioned near the bottom of the cell. The assembly finally was raised around the shaft of the RRDE already mounted on a rotator, maintaining a continuous N_2 flow through the cell. Freedom from dioxygen contaminant was verified by cyclic voltammetry before each RRDE experiment. The RRDE had a 4.8-mm-diameter glassy-carbon disk, a 0.22-

(9) Johnson, E. C.; Meyer, T. J.; Winterton, N. *Inorg. Chem.* **1971**, *10*, 1673.
(10) Connelly, N. G.; Geiger, W. E. *Adv. Organomet. Chem.* **1984**, *23*, 1.
(11) Pugh, J. R.; Meyer, T. J. *J. Am. Chem. Soc.* **1988**, *110*, 8245.
(12) Davies, S. G.; Simpson, S. J.; Parker, V. D. *J. Chem. Soc., Chem. Commun.* **1984**, 353.
(13) Dessy, R. E.; Weissman, P. M.; Pohl, R. L. *J. Am. Chem. Soc.* **1966**, *88*, 5117.
(14) Legzdins, P.; Wassnik, B. *Organometallics* **1984**, *3*, 1811.
(15) Miholová, D.; Vlcek, A. A. *Inorg. Chim. Acta* **1980**, *41*, 119.
(16) Morán, M.; Cuadrado, I.; Losada, J. *J. Organomet. Chem.* **1987**, *320*, 317.
(17) Ellis, J. *J. Organomet. Chem.* **1975**, *86*, 1.
(18) Gladysz, J. A.; Williams, G. M.; Tam, W.; Johnson, D. L.; Parker, D. W.; Selover, J. C. *Inorg. Chem.* **1979**, *18*, 553.
(19) Gansow, O. A.; Burke, A. R.; Vernon, W. D. *J. Am. Chem. Soc.* **1976**, *98*, 5817.
(20) Adams, R. D.; Cotton, F. A. *J. Am. Chem. Soc.* **1973**, *95*, 6589.
(21) Bullitt, J. G.; Cotton, F. A.; Marks, T. J. *J. Am. Chem. Soc.* **1970**, *92*, 2155.
(22) Amatore, C.; Savéant, J. M. *Electroanal. Chem.* **1977**, *85*, 27.
(23) Shriver, D. F.; Drezdzon, M. A. *The Manipulation of Air Sensitive Compounds*; John Wiley and Sons: New York, 1986.
(24) Gordon, A. J.; Ford, R. A. *The Chemist's Companion*; John Wiley and Sons: New York, 1972.

mm-wide Pt ring, and a 0.19-mm disk-ring gap. Rotation rates ranged from 500 to 6000 rpm. $[Fe(CO)_2(\eta^5\text{-}Cp)]_2$ cyclic voltammetry is the same on glassy-carbon and Pt electrodes. In the kinetic measurements, E_{disk} was scanned from −1.5 to −2.1 V vs SCE with E_{ring} held at −1.5 V (at −22 °C) or at −1.3 V (for $T < -22$ °C, to overcome solution resistance).

The required[25] dimer diffusion coefficients at lowered temperatures were determined by chronoamperometry and steady-state voltammetry at a 10-μm-diameter Pt microelectrode by using decamethylferrocene as a model compound. Solution kinematic viscosities at each temperature were measured with an Ostwald viscometer.

Double Potential Step Chronoamperometry (DPSCA). A known volume of THF or propionitrile was vacuum-transferred into the electrochemical cell (through a screw type side-arm valve) previously charged with samples of dry electrolyte (Bu_4NPF_6) and metal dimer, the latter placed in a side-arm chamber. The electrolyte solution was deoxygenated with three freeze–pump–thaw cycles and cooled to the desired temperature, and a series of background current DPSCA transients were recorded. Subsequently, the metal dimer was introduced from the side-arm chamber, and an identical series of DPSCA transients were recorded, from which the background currents were subtracted by using a microcomputer.

In a typical DPSCA experiment with $[Fe(CO)_2(\eta^5\text{-}Cp)]_2^-$ propionitrile solutions, the (0.0032 cm^2) Pt electrode starting potential was −1.1 V vs SCE (insufficiently negative to reduce the dimer). The potential was stepped to −2.1 V vs SCE (sufficiently negative to overcome the solution resistance and reduce the dimer) and after a time τ_{exp} returned to the starting potential. At each temperature, a series of DPSCA measurements were conducted, by using τ_{exp} values spanning several orders of magnitude, to assure that at least one τ_{exp} value was near the lifetime of the $[Fe(CO)_2(\eta^5\text{-}Cp)]_2^{\bullet-}$ intermediate. Between experiments, the electrode was held at 0.0 V vs SCE to clear the solution around the electrode of residual $[Fe(CO)_2(\eta^5\text{-}Cp)]^-$ anion.

DPSCA measurements in propionitrile of $[Fe(CO)_2(\eta^5\text{-}Cp^*)]_2$ and $[Ru(CO)_2(\eta^5\text{-}Cp)]_2$ encountered difficulties with excessive background currents in that solvent, so these dimers were studied in THF solutions by using a starting potential of −1.8 V and reducing potentials of −2.3 and −2.7 V vs SCE, respectively.

Results

Cyclic Voltammetry. Cyclic voltammetry was used to map out the kinetic behavior of the three metal dimers from room temperature to −76 °C. Voltammograms of $[Fe(CO)_2(\eta^5\text{-}Cp)]_2$ at temperatures above −25 °C (Figure 2, top) show an irreversible reduction wave a followed on the reverse potential sweep by an irreversible oxidation wave b at a more positive potential. As the temperature is lowered, oxidation wave b is gradually replaced with an oxidation, wave c, at less positive potential, that is an obvious partner of the reduction wave a. The change is nearly complete at −76 °C.

Figure 2 (bottom) compares the reduction (a) and oxidation (d) waves of $[Fe(CO)_2(\eta^5\text{-}Cp)]_2$ at room temperature and at −76 °C. At room temperature, the peak currents of waves a and d are roughly equal (5.3 μA vs 6.3 μA, respectively) as expected, since both processes have been shown to be (net) two-electron reactions (via bulk electrolysis[8]). At −76 °C, on the other hand, the peak current of reduction wave a, 1.8 μA, is only about half (58%) that of the oxidation wave (3.1 μA). Taking the oxidation wave as an internal two-electron standard, this result indicates that the reduction decreases from a two-electron to an almost[26] one-electron process at lowered temperature.

Our interpretation of these observations follows that of Parker and co-workers.[12] At room temperature, wave a corresponds to a net two-electron reduction involving rapid (on the potential sweep time scale) dissociation of an initially produced dimer radical anion into a mononuclear $[Fe(CO)_2(\eta^5\text{-}Cp)]^-$ anion and a further reducible $[Fe(CO)_2(\eta^5\text{-}Cp)]^\bullet$ radical. The two $[Fe(CO)_2(\eta^5\text{-}Cp)]^-$ anions thus produced are reoxidized at the potential of wave b. The $[Fe(CO)_2(\eta^5\text{-}Cp)]^\bullet$ radical product of wave b evidently redimerizes very rapidly, since no reduction counterpart (the $[Fe(CO)_2(\eta^5\text{-}Cp)]^{\bullet/-}$ couple) of wave b is observed. (Parker and co-workers[12] show a voltammogram with a $[Fe(CO)_2(\eta^5\text{-}Cp)]^\bullet$ reduction wave but on the other hand used a Hg electrode onto which adsorption was noted.) Rapid redimerization of $[Fe(CO)_2(\eta^5\text{-}Cp)]^\bullet$ is, in fact, expected given a photochemical estimation[4] of a rate constant of 10^9 M^{-1} s^{-1}.

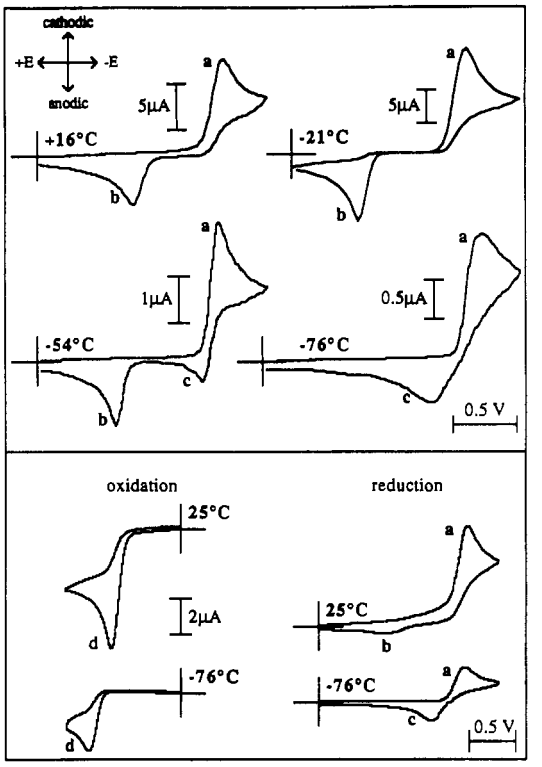

Figure 2. Cyclic voltammetry of $[Fe(CO)_2(\eta^5\text{-}Cp)]_2$ in 0.1 M Bu_4NPF_6/propionitrile. Top panel: +16 and −76 °C (250 mV/s, 5.4 mM $[Fe(CO)_2(\eta^5\text{-}Cp)]_2$); −21 °C (300 mV/s, 8.9 mM $[Fe(CO)_2(\eta^5\text{-}Cp)]_2$); −54 °C (250 mV/s, 6.0 mM $[Fe(CO)_2(\eta^5\text{-}Cp)]_2$). Bottom panel: oxidation (left) and reduction (right) voltammograms for 3.3 mM $[Fe(CO)_2(\eta^5\text{-}Cp)]_2$ at room temperature (100 mV/s) and −76 °C (400 mV/s). The electrode area is 0.0032 cm^2; the potential axis origin is at −0.3 V vs SCE.

At lower temperatures, the dimer dissociation reaction becomes quenched and waves a and c approach the one-electron reduction of $[Fe(CO)_2(\eta^5\text{-}Cp)]_2$ and oxidation of its radical-anion $[Fe(CO)_2(\eta^5\text{-}Cp)]_2^{\bullet-}$. Wave b is correspondingly diminished. The cyclic voltammetry in Figure 2 supports the interpretation that the two-electron reduction of $[Fe(CO)_2(\eta^5\text{-}Cp)]_2$ does not proceed by reactions 2 and 3 but rather by a sequence of a one-electron reduction and dissociation and a second electron, i.e., an "ECE" sequence[22] as in reactions 4–7.

The temperature dependence of the cyclic voltammetry of $[Fe(CO)_2(\eta^5\text{-}Cp^*)]_2$ (Figure 3) is analogous to that of $[Fe(CO)_2(\eta^5\text{-}Cp)]_2$, except that wave c appears at a higher temperature (0 °C) and that wave b for the oxidation of $[Fe(CO)_2(\eta^5\text{-}Cp^*)]_2^{\bullet-}$ vanishes at a higher temperature (−53 °C). This means that cleavage of the $[Fe(CO)_2(\eta^5\text{-}Cp^*)]_2^{\bullet-}$ dimer radical anion is more readily thermally quenched than $[Fe(CO)_2(\eta^5\text{-}Cp)]_2^{\bullet-}$; i.e., the radical anion of $[Fe(CO)_2(\eta^5\text{-}Cp^*)]_2$ is more stable than that of $[Fe(CO)_2(\eta^5\text{-}Cp)]_2$.

We were not successful in producing analogous changes in the cyclic voltammetry of the ruthenium dimer $[Ru(CO)_2(\eta^5\text{-}Cp)]_2$. Figure 4 shows that the two-electron $[Ru(CO)_2(\eta^5\text{-}Cp)]_2$ reduction (a) and the $[Ru(CO)_2(\eta^5\text{-}Cp)]^{\bullet-}$ oxidation (b) waves persist in voltammetry at −76 °C, the lowest temperature examined. Thus, the dissociation of reduced $[Ru(CO)_2(\eta^5\text{-}Cp)]_2$ dimer is much more rapid than that of the two iron dimer complexes. (We note at this point that $[Ru(CO)_2(\eta^5\text{-}Cp)]_2$ is also more rapidly fluxional than the iron dimers.) Strictly speaking, the data do not reveal whether $[Ru(CO)_2(\eta^5\text{-}Cp)]_2$ reduction follows the two-electron

(25) Bard, A. J.; Faulkner, L. R. *Electrochemical Methods*; John Wiley and Sons: New York, 1980.

(26) Ideally, a one-electron reduction wave peak current is 36% of that of a two-electron oxidation peak current; the slightly higher ratio observed suggests that, at this temperature, either passage of the second electron in the reduction step is not entirely quenched or passage of the second electron in the oxidation is partially quenched.

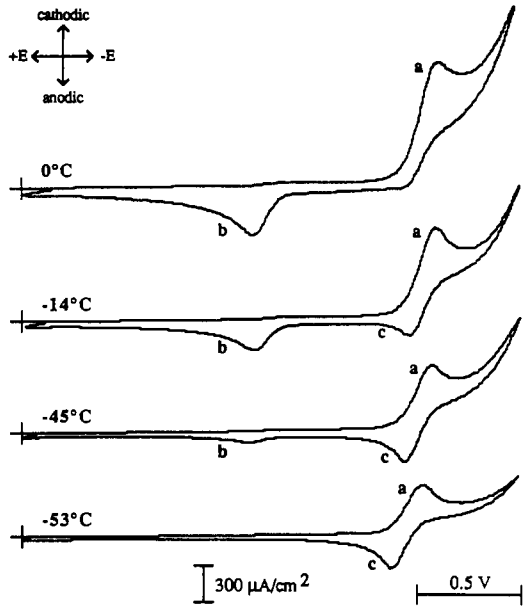

Figure 3. Cyclic voltammetry of 1.9 mM $[Fe(CO)_2(\eta^5\text{-}Cp^*)]_2$ in 0.1 M Bu_4NPF_6/THF at indicated temperatures. The scan rate is 200 mV/s; the potential axis origin is at −0.3 V vs SCE.

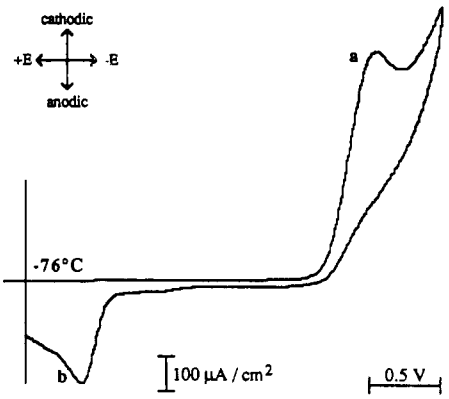

Figure 4. Cyclic voltammetry of 3.8 mM $[Ru(CO)_2(\eta^5\text{-}Cp)]_2$ at −76 °C in 0.1 M Bu_4NPF_6/THF. The scan rate is 200 mV/s; the potential axis origin is at −0.3 V vs SCE.

pathway of reactions 2 and 3 or the ECE pathway of reactions 4–7, but if analogy with the iron dimers has any merit, the latter is more likely.

Double Potential Step Chronoamperometry. Electrochemical reaction reversal methods[27,28] probe dimer radical anion dissociation kinetics by generating it, allowing it to react for a period of time (i.e., undergo cleavage), and then assessing the quantity of unreacted radical anion by reoxidizing it. In DPSCA, the electrode potential is held at a reducing value for a time, τ_{exp}, after which it is readjusted to an oxidizing value. The appropriate theory for the current transients has to account for both diffusion and chemical reaction rates. The theory by Schwartz and Shain[28] was originally developed for a first-order E_rC_i mechanism but is appropriate for the ECE mechanism when the chemical step (reaction 5) is rate determining and reaction 6 is negligible compared to the fast homogeneous-phase reaction 7. This situation is the so-called "DISP1" variation of the ECE mechanism,[22] which also exhibits first-order behavior and for which the observed first-order rate constant, k_{obs}, is simply twice that (k_1) of reaction 5.

Figure 5A shows a typical DPSCA reduction–oxidation current transient (—) for $[Fe(CO)_2(\eta^5\text{-}Cp)]_2$ in propionitrile, with a reduction step time τ_{exp} = 0.10 s. The current at $t > \tau_{exp}$ corresponds to reoxidation of the surviving dimer radical anion. The background current (Figure 5A), which is significant during both time periods, was measured in blank electrolyte solution and subtracted from the total current prior to analysis of the data.

In the data analysis, oxidation currents $i(t + \tau_{exp})$, measured at time t following τ_{exp}, are compared to reduction currents $i(t)$ measured at time t during the reducing potential step. Such current ratios, $i(t + \tau_{exp})/i(t)$, are shown in Figure 5B as a function of the fraction of the step time τ_{exp} that the measurement time, t, represents. The theory for such a plot[28] is

$$-i(t + \tau_{exp})/i(t) = \phi[k_{obs}, \tau_{exp}, t] - [(t/\tau_{exp})/(1 + t/\tau_{exp})]^{1/2} \quad (8)$$

where ϕ is a numerically evaluated function.[28] The theory–experiment comparison is conducted by seeking a rate constant k_{obs} that with eq 8 predicts a current ratio that agrees with experiment over the entire range of kinetic times t/τ_{exp}. Figure 5B shows that this can be done; a theoretical curve for k_{obs} = 10.5 s^{-1} fits the −44 °C experimental results of Figure 5A quite well. The good agreement in Figure 5B was typical of experimental results at other temperatures for $[Fe(CO)_2(\eta^5\text{-}Cp)]_2$ and for the cleavage kinetics of $[Fe(CO)_2(\eta^5\text{-}Cp^*)]_2$, as long as the chosen step time, τ_{exp}, was within a factor of 4 of the reaction half-life ($1/k_{obs}$) of the dimer radical anion. Longer or shorter τ_{exp} values produced less good fits; it is well-known that electrochemical kinetic measurements are most accurate when the experimental and reaction time scales are similar.[25,28]

Table I. DPSCA Results for Reductive Cleavage of Metal Dimers[a]

metal dimer syst	temp, °C	concn of dimer, mM	$k_{obs} = 2k_1$, s^{-1}
$[Fe(CO)_2(\eta^5\text{-}Cp)]_2$	−23	1.3	172 (±12)[b]
in propionitrile	−23	3.6	175 (±10)
(0.1 M Bu_4NPF_6)	−23	8.9	180 (±27)
	−44	4.6	10.5 (±0.5)
	−50	8.0	7.9 (±0.8)
	−55	6.0	2.8 (±1.0)
	−66	1.4	0.49 (±0.03)
	−66	3.7	0.52 (±0.01)
	−66	6.0	0.54 (±0.01)
	−78	5.4	0.090 (±0.014)
$[Fe(CO)_2(\eta^5\text{-}Cp^*)]_2$	0	1.3	7.0 (±1.7)
in THF	−22	6.6	1.9 (±0.4)
(0.1 M Bu_4NPF_6)	−42	4.7	0.22 (±0.03)

[a] Each k_{obs} derived from a series of DPSCA experiments by using a wide range of step times (τ_{exp}); reported value of k_{obs} is an average of ≥30 $i(t + \tau_{exp})/i(t)$ points taken in an experiment where τ_{exp} was close to $(1/k_{obs})$ and from the part of the experiment with best S/N ratio, $0.2 \le (t/\tau_{exp}) \le 0.6$. [b] Reported error represents a 68% confidence interval.

Table II. Metal Dimer Radical Anion Cleavage Kinetic and Activation Data

solvent (0.1 M Bu_4NPF_6)	expt type[a]	k_1(0 °C),[b] s^{-1}	E_A,[c] kcal/mol	$\Delta S^{\ddagger}$,[d] cal/mol
		$[Fe(CO)_2(\eta^5\text{-}Cp)]_2$		
acetonitrile[e]	DCV	1060	16	11
propionitrile	DPSCA	718	14 (±4)[f]	16 (±4)
butyronitrile	RRDE	641	12 (±5)[f]	11 (±4)
		$[Fe(CO)_2(\eta^5\text{-}Cp^*)]_2$		
THF	DPSCA	7.0	10 (±8)[f]	−6 (±4)
		$[Ru(CO)_2(\eta^5\text{-}Cp)]_2$		
THF	DPSCA	>1000[g] at (−77 °C)		

[a] DCV, DPSCA, and RRDE are derivative cyclic voltammetry, double potential step chronoamperometry, and rotated ring–disk electrochemistry, respectively. [b] Rate extrapolated to 0 °C by using an Arrhenius plot. [c] From Arrhenius plot of data in Tables I and III. [d] From ln $[k_1/T]$ vs $1/T$ intercept of Eyring plot of data in Tables I and II. [e] From ref 12. [f] $\Delta H^{\ddagger}$ values from Eyring plots are 14, 13, and 11 kcal/mol, respectively. [g] Lower limit, estimated at −77 °C; for comparison, k_1 = 0.045 s^{-1} for $[Fe(CO)_2(\eta^5\text{-}Cp)]_2$ at this temperature.

(27) Hanafey, M. K.; Scott, R. L.; Ridgeway, T. H.; Reilley, C. N. *Anal. Chem.* **1977**, *50*, 116.
(28) Schwartz, W. M.; Shain, I. *J. Phys. Chem.* **1965**, *69*, 30.

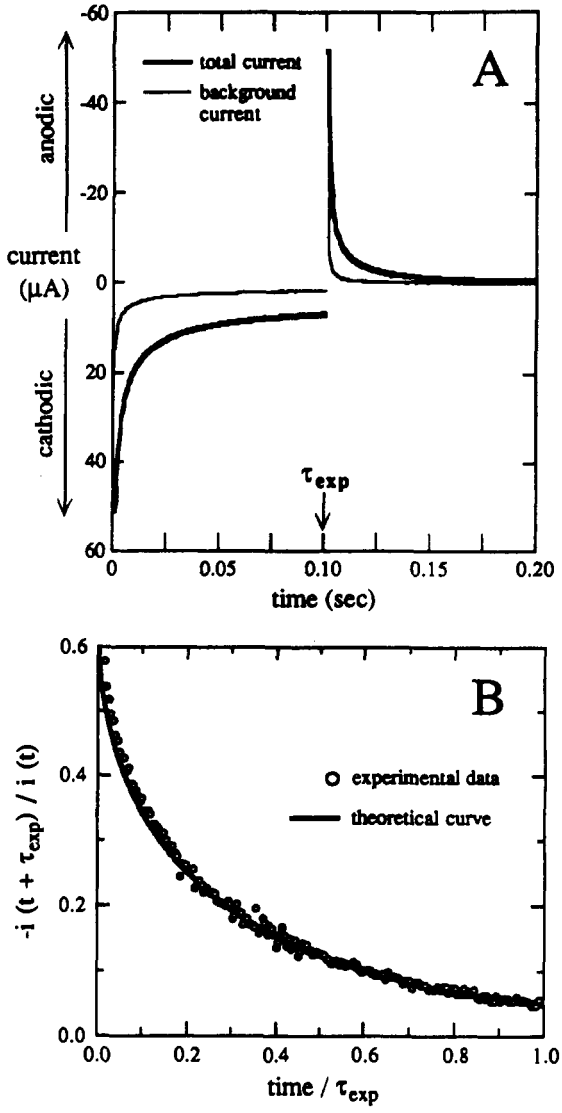

Figure 5. Double potential step chronoamperometry of 4.6 mM [Fe(CO)$_2$(η^5-Cp)]$_2$ in 0.1 M Bu_4NPF_6/propionitrile at −43 °C. Step time τ_{exp} = 0.1 s. Panel A: Current transients for potential step from −0.8 to −1.9 V in blank electrolyte solution (thin line) and with added [Fe(CO)$_2$(η^5-Cp)]$_2$ (dark line). Panel B: Ratio of experimental currents $-i(t + \tau_{exp})/i(t)$ for $0 < t < \tau_{exp}$ versus normalized time (t/τ_{exp}) compared to theory (solid line) for k_{obs} = 10.5 s^{-1}. Electrode area equals 0.0032 cm^2.

Table I lists thus-derived DPSCA cleavage rate constants as a function of temperature for anion dimers [Fe(CO)$_2$(η^5-Cp*)]$_2^{\bullet-}$ and [Fe(CO)$_2$(η^5-Cp)]$_2^{\bullet-}$ and as a function of concentration for [Fe(CO)$_2$(η^5-Cp)]$_2^{\bullet-}$. k_1 is independent of reactant concentration, consistent with a first-order process and with the ruling out of reaction 7 as a rate-controlling step. The rate constants are plotted in Arrhenius fashion in Figure 6, and activation parameters are summarized in Table II.

DPSCA experiments performed at −77 °C with the ruthenium dimer failed to detect any wave c reoxidation current above background following the positive potential step. We estimate, from the sensitivity of the measurement, that at −77 °C the upper limit of the [Ru(CO)$_2$(η^5-Cp)]$_2^{\bullet-}$ dimer radical anion lifetime is less than 1 ms, corresponding to $k_{obs} > 1000$ s^{-1} in 0.1 M Bu_4NPF_6/THF. This rate constant is more than 4 orders of magnitude larger than that of [Fe(CO)$_2$(η^5-Cp*)]$_2^{\bullet-}$ (Table I, k_{obs} = 0.09 s^{-1}) at the same temperature in propionitrile solution.

Rotated Ring–Disk Electrode Voltammetry. Any kinetics investigation is strengthened when different experimental approaches give equivalent results; here, RRDE results support those from DPSCA. RRDE voltammetry[25] relies on a steady (as opposed to transient as in DPSCA) generation of the [Fe(CO)$_2$(η^5-Cp)]$_2^{\bullet-}$ radical anion at the disk electrode. The radical anion is hydrodynamically swept (at a velocity determined by the electrode rotation rate) across the gap to the ring electrode, where it is reoxidized at a steady ring potential E_{ring}. The gap-crossing time is decreased by faster electrode rotation rates and is equivalent, in a kinetic sense, to the step time τ_{exp} in DPSCA.

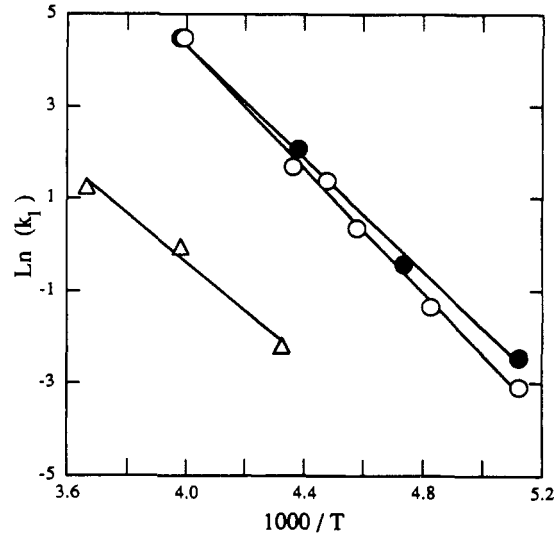

Figure 6. Arrhenius plots for the dissociation of iron dimer anion radicals. For [Fe(CO)$_2$(η^5-Cp)]$_2^{\bullet-}$ results are from DPSCA (○) and RRDE (●) in propionitrile and butyronitrile, respectively. For [Fe(CO)$_2$(η^5-Cp*)]$_2^{\bullet-}$, results are from DPSCA (△) in THF. Kinetic data are from Tables I and III; activation parameters are listed in Table II.

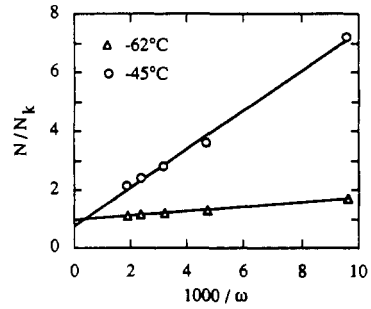

Figure 7. Typical plots of collection efficiency ratio (N/N_k) vs ($1000/\omega$) from RRDE experiments with [Fe(CO)$_2$(η^5-Cp)]$_2$ in 0.1 M Bu_4NPF_6/butyronitrile at −42 and −62 °C. RRDE electrode collection efficiency for k_{obs} = 0 is N = 0.240. ω is in rads/s.

Even in the absence of chemical reactions, the current at the ring is less than that at the disk; this rotation rate-independent "collection efficiency", $N = -i_{ring}/i_{disk}$, is a property solely of the particular ring, disk, and gap dimensions. For the electrode employed here, N = 0.240, as determined with ferrocene(0/1+) as a stable redox couple. A smaller collection efficiency N_k is observed upon reducing [Fe(CO)$_2$(η^5-Cp)]$_2$ at the disk electrode, when E_{ring} is set to reoxidize [Fe(CO)$_2$(η^5-Cp)]$_2^{\bullet-}$ but not [Fe(CO)$_2$(η^5-Cp)]$^-$. N_k thus reflects the extent of [Fe(CO)$_2$(η^5-Cp)]$_2^{\bullet-}$ cleavage during gap-crossing, according to the relation[25]

$$N/N_k = 1 + 1.28(\kappa^{1/3}k_{obs}/D^{1/3}\omega) \qquad (9)$$

where κ and D, respectively, are the kinematic viscosity of the solvent and the diffusion coefficient of the dimer. Equation 9 is formally for an E_rC_i process but applies to the present ECE (DISP1) reaction scheme because the overall behavior of the latter is also first order, with k_{obs} being simply $2k_1$ for reaction 5.

The RRDE measurements were carried out by slowly varying E_{disk} from −1.5 to −2.1 V vs SCE (i.e., to the plateau of wave a), while E_{ring} is maintained at −1.3 V (the plateau of wave c). Both disk and ring currents rise to steady-state plateaus at the most negative E_{disk}. The N/N_k ratio varies with rotation rate at −45 and at −63 °C, as shown in Figure 7; the plots are linear and extrapolate to near-unity N/N_k at infinite rotation rate, as expected

Table III. RRDE Results from Reductive Cleavage of $[Fe(CO)_2(\eta^5\text{-Cp})]_2$ in 0.1 M Bu_4NPF_6/Butyronitrile

temp, °C	κ,[a] stokes	D,[b] 10^{-7} cm²/s	$k_{obs} = 2k_1$, s^{-1}
−22	0.0136	12.7	176 (±9)
−45	0.0253	7.03	15.5 (±0.7)
−62	0.0355	4.20	1.29 (±0.09)
−78	0.0748	2.38	0.17 (±0.05)

[a] Kinematic viscosity measured with Ostwald viscometer in a constant-temperature bath. [b] Diffusion coefficients for the model compound decamethylferrocene, from chronoamperometry and microelectrode voltammetry.

from the theory. Rate constants derived from these results and those at other temperatures are listed in Table III. Activation parameters derived from an Arrhenius plot (Figure 6) are given in Table II. The rate constants and activation parameters from RRDE are in excellent agreement with the DPSCA results (see Table II).

The RRDE voltammetry also verified the electron stoichiometry of waves b and c in Figure 2 with respect to that of wave a for the reduction of $[Fe(CO)_2(\eta^5\text{-Cp})]_2$. Waves b and c are both one-electron reactions (oxidations of $[Fe(CO)_2(\eta^5\text{-Cp})]^-$ and $[Fe(CO)_2(\eta^5\text{-Cp})]_2^{\bullet-}$, respectively), and so although their relative sizes can vary with temperature and rotation rate, their sum should ideally represent a total recovery of the two electrons passed in wave a. This was examined by scanning E_{disk} from −1.5 to −2.1 V (vs SCE) while E_{ring} was maintained at −0.3 V, which should drive the oxidation reactions of *both* waves b and c, collecting both mononuclear $[Fe(CO)_2(\eta^5\text{-Cp})]^-$ and dimer $[Fe(CO)_2(\eta^5\text{-Cp})]_2^{\bullet-}$ at the ring. A collection efficiency of 0.24 was observed at −45 and at −78 °C, identical with that measured by using ferrocene, demonstrating a full recovery of charge and the absence of other decay pathways for these two species.

Discussion

The results for $[Fe(CO)_2(\eta^5\text{-Cp})]_2$ agree with those of Parker and co-workers[12] in that the overall two-electron pathway proceeds through heterolytic cleavage of the radical anion and the second electron is added to the $[Fe(CO)_2(\eta^5\text{-Cp})]^\bullet$ radical. We have established that the same reaction pathway applies to the (pentamethylcyclopentadienyl)iron dimer $[Fe(CO)_2(\eta^5\text{-Cp}^*)]_2$. Both dimers cleave in a first-order reaction step, as shown by satisfactory fit of kinetic data to a first-order theory and by agreement between both rate constants and activation parameters for $[Fe(CO)_2(\eta^5\text{-Cp})]_2$ as obtained from DPSCA and RRDE experiments. A mechanism consistent with these observations is the ECE (DISP1) pathway[22] where $k_2 \gg k_1$ and reaction 6 does not significantly compete with reaction 7.

The ruthenium dimer $[Ru(CO)_2(\eta^5\text{-Cp})]_2$ undergoes a much more rapid dissociation upon reduction, and strictly speaking, the reaction pathway is not defined by the experimental results. We will suppose, however, that the ruthenium dimer also follows the radical anion cleavage pathway by drawing analogy to the iron dimer chemistry and by also recalling that (in the absence of intramolecular rearrangements, which produce much better electron acceptors) Coulombic effects typically require application of a more negative potential to pass the second electron. If this supposition is made, the rate constant for cleavage of the $[Ru(CO)_2(\eta^5\text{-Cp})]_2^{\bullet-}$ radical anion is more than 10^2-fold larger than that for the radical anion of $[Fe(CO)_2(\eta^5\text{-Cp})]_2$, which in turn (Table II) is 10^2 larger than that for the radical anion of $[Fe(CO)_2(\eta^5\text{-Cp}^*)]_2$. That is, very large differences in chemical reactivity exist between the radical anions of these three dimers.

Inspection of the results in Table II reveals that rate constants, activation barriers, and activation entropies for $[Fe(CO)_2(\eta^5\text{-Cp})]_2$ from DPSCA, RRDE, and derivative cyclic voltammetry[12] are in reasonably good agreement with one another. In the case of the more slowly cleaving $[Fe(CO)_2(\eta^5\text{-Cp}^*)]_2^{\bullet-}$ radical anion, for which no prior data exist, the measured activation barrier is not very different from that for $[Fe(CO)_2(\eta^5\text{-Cp})]_2^{\bullet-}$, but the activation entropy, even after accounting for the considerable experimental uncertainty, is noticeably less and apparently negative. That is, the lower cleavage reactivity of the $[Fe(CO)_2(\eta^5\text{-Cp}^*)]_2^{\bullet-}$ radical anion appears to be associated with an unfavorable entropy of activation term.

Let us now consider how these kinetic details can be used to infer chemical events associated with the dimer cleavage and possible reasons for the substantial reactivity difference between the three metal dimer radical anions. An important distinction is whether the measured rate constant k_{obs} reflects the rate of dimer cleavage into mononuclear complexes (reaction 5) or instead reflects the rate of a reaction step intervening between dimer radical anion formation (reaction 4) and the actual cleavage step (reaction 5). This second possibility, which will be referred to as *cleavage-precursor* rate control, has not to our knowledge been previously addressed in the literature[6-18] dealing with reduction or oxidation of these dimers. Given that the dimers are multiply CO-bridged, some form of internal reorganization must in fact precede attainment of the structural form most prone to dimer dissociation. For example, the pairwise opening of CO bridges that has been proposed for the cis–trans isomerization pathway[20] leads to a non-CO-bridged isomer whose already weak[29] Fe–Fe bond would be further weakened in the dimer radical anion by addition of an electron to the Fe–Fe σ^* LUMO.[30]

A primary issue then is whether intramolecular cleavage-precursor reaction or actual dimer cleavage (reaction 5) is overall rate controlling. This requires consideration of their differing electronic structures and isomerization dynamics, for which the available information is unfortunately not complete. Not only are the reasons for the differing photoreactivities[5] and isomerization rates[19-21] of the different $[Fe(CO)_2(\eta^5\text{-Cp})]_2$, $[Fe(CO)_2(\eta^5\text{-Cp}^*)]_2$, and $[Ru(CO)_2(\eta^5\text{-Cp})]_2$ isomers not well understood, but the most pertinent electronic and isomerization rate comparison[31] would not be of them but of their dimer radical anions, about which such information is lacking.

The following discussion of evidence bearing on cleavage-precursor rate control is based on the (substantial) assumption that isomerization rates for a dimer and for its radical anion are similar. First, examination of NMR-based isomerization rate data[19] for $[Fe(CO)_2(\eta^5\text{-Cp})]_2$ and $[Ru(CO)_2(\eta^5\text{-Cp})]_2$ shows that isomerization interconversion (i.e., bridging CO bond breaking) is much more facile for $[Ru(CO)_2(\eta^5\text{-Cp})]_2$. Second, at −77 °C, the NMR[19] results indicate a cis/trans interconversion rate of 3×10^4 s^{-1} for $[Ru(CO)_2(\eta^5\text{-Cp})]_2$; such a rate is consistent with the electrochemical results (Table II) in that it should be undetectable on our measurement time scale. Third, for $[Fe(CO)_2(\eta^5\text{-Cp})]_2$ the NMR[19] bridge/terminal carbonyl exchange rate and activation barrier are k(−66 °C) = 0.94 s^{-1} and E_A = 11.2 kcal/mol, which are close to the results for $[Fe(CO)_2(\eta^5\text{-Cp})]_2$ (k(−66 °C) = 0.54 s^{-1} and E_A = 12–14 kcal/mol). Fourth, while there are no isomerization rate data for $[Fe(CO)_2(\eta^5\text{-Cp}^*)]_2$, the effect of a single methyl substituent seems to be to slow[19] the isomerization rate, and the radical anion of $[Fe(CO)_2(\eta^5\text{-Cp}^*)]_2$ indeed in the present study is the most slowly reacting of the three. Its ΔS^* is negative (Table II); while negative activation entropies[32] are known for other organometallic cleavage reactions, this is not consistent with a dissociative process like reaction 5. On the other hand, spectroscopic data[33] provides a strictly electronic reason for greater stability in the case of $[Fe(CO)_2(\eta^5\text{-Cp}^*)]_2$ in its lower energy $\sigma \rightarrow \sigma^*$ transition (λ = 364 nm, THF, 25 °C) compared to $[Fe(CO)_2(\eta^5\text{-Cp})]_2$ (λ = 344 nm, THF, 25 °C). Finally, while the above points are suggestive of the importance of cleavage-

(29) Jemmis, E. D.; Pinhas, A. R.; Hoffmann, R. *J. Am. Chem. Soc.* **1980**, *102*, 2576.
(30) Bursten, B. E.; Cayton, R. H.; Gatter, M. G. *Organometallics* **1988**, *7*, 1342.
(31) We note that isomerization among *parent* dimers *prior* to transfer of the first electron may occur, but the electrochemical measurement shows no evidence of limitation of the rate of reduction of dimer by such kinetics.
(32) Ikeshoji, T.; Parker, V. D. *Acta Chem. Scand.* **1983**, *B37*, 715.
(33) Wavelengths are from our own UV–vis survey of the iron dimers in THF solutions at room temperature. Assignments are based on ref 5 although others have been offered in ref 1.

precursor steps, we emphasize that they are based on assuming similar isomerization dynamics for dimer and its radical anion. Further and more structurally explicit data, such as could come from infrared spectroelectrochemistry, is obviously needed in future investigations.

Finally, we should note that these results are a further example of using cryoelectrochemistry[34-36] to probe chemical reactivities too rapid to observe at room temperature. Recently, we extended[37] the accessible voltammetric temperature range down to 88 K using a new low-melting electrolyte solution. While the full range of temperatures made available by this development is not exploited here, we suggest that cryoelectrochemistry will prove a useful supplement to ultrafast microelectrode voltammetry[38-42] in observing facile chemical reactions and, as in the present case, add significant activation parameter information.

Acknowledgment. This research was supported in part by grants from the National Science Foundation and the Office of Naval Research. We are grateful for useful comments by Professors M. S. Brookhart and T. J. Meyer.

(34) Stone, N. J.; Sweigart, D. A.; Bond, A. M. *Organometallics* **1986**, *5*, 2553.
(35) O'Connell, K. M.; Evans, D. H. *J. Am. Chem. Soc.* **1983**, *105*, 1473.
(36) Van Duyne, R. P.; Reilley, C. N. *Anal. Chem.* **1972**, *44*, 142.
(37) McDevitt, J. T.; Ching, S.; Sullivan, M.; Murray, R. W. *J. Am. Chem. Soc.* **1989**, *111*, 4528.
(38) Howell, J. O.; Kuhr, W. G.; Ensman, R. E.; Wightman, R. M. *J. Electroanal. Chem. Interfacial Electrochem.* **1986**, *209*, 77.
(39) Howell, J. O.; Wightman, R. M. *J. Phys. Chem.* **1984**, *88*, 3918.
(40) Pierce, D. T.; Geiger, W. E. *J. Am. Chem. Soc.* **1989**, *111*, 7636.
(41) Andrieux, C. P.; Hapiot, P.; Savéant, J. M. *J. Phys. Chem.* **1988**, *92*, 5992.
(42) Baer, C. D.; Camaioni-Neto, C. A.; Sweigart, D. A.; Bond, A. M.; Mann, T. F.; Tondreau, G. A. *Coord. Chem. Rev.* **1989**, *93*, 1.

Contribution from the Department of Chemistry, Gorlaeus Laboratories, Leiden University, P.O. Box 9502, 2300 RA Leiden, The Netherlands

Reactivity of Chloro- and Aqua(diethylenetriamine)platinum(II) Ions with Glutathione, *S*-Methylglutathione, and Guanosine 5′-Monophosphate in Relation to the Antitumor Activity and Toxicity of Platinum Complexes

Milos I. Djuran,† Edwin L. M. Lempers, and Jan Reedijk*

Received October 23, 1990

The reactivity of the two platinum(II) complexes $[Pt(dien)Cl]^+$ and $[Pt(dien)(H_2O)]^{2+}$ with glutathione (GSH), *S*-methylglutathione (GS-Me), and guanosine 5′-monophosphate (5′-GMP) has been investigated and compared. The reactions of GSH and GS-Me with the two platinum complexes are second order, i.e. with a direct nucleophilic attack by the entering ligand on the platinum. For the reaction of 5′-GMP with $[Pt(dien)Cl]^+$ the rate-determining step is the formation of $[Pt(dien)(H_2O)]^{2+}$ followed by a rapid nucleophilic substitution of 5′-GMP, through its N7 atom. The kinetic data show that 5′-GMP has a strong kinetic preference for $[Pt(dien)(H_2O)]^{2+}$ compared with GSH and GS-Me. On the contrary, $[Pt(dien)Cl]^+$ reacts more rapidly with GSH and GS-Me. The obtained kinetic data have been analyzed in relation to the antitumor activity and toxicity of platinum complexes. As a result, a new strategy for the development of novel platinum drugs with improved antitumor properties and lower toxicities has been suggested.

Introduction

After Rosenberg's discovery[1] of the antitumor activity of [*cis*-$PtCl_2(NH_3)_2$] complex (abbreviated cisplatin), many other platinum(II) complexes have been synthesized and tested with the major aims of obtaining better antitumor activity, increased solubility, and lower toxic side effects. At the same time extensive research has been done to establish the mechanism of antitumor activity and toxicity of such platinum(II) complexes.

It has now been generally accepted that the chloro hydrolysis is the rate-determining step in the reaction of cisplatin with DNA.[2] Concerning the rate-determining step of platinum amine compounds with sulfur-containing biomolecules, the available data are rather controversial. It has been reported that the chloro hydrolysis is the rate-determining step in the reactions of cisplatin with leucine aminopeptidase,[3] γ-glutamyl transpeptidase,[3,4] and albumin.[5] However, it has also been suggested that there may be a direct binding to proteins without prior aquation,[6] as has been observed with cysteine,[7,8] glutathione,[7,8] adenosine triphosphatase,[3] and with metallothionein.[9] Given the importance of sulfur-containing biomolecules and their likely responsibility for the development of resistance, inactivation, and toxic side effects of cisplatin, it appears necessary to establish the details of their mechanism of reactions with platinum complexes.

Scheme I

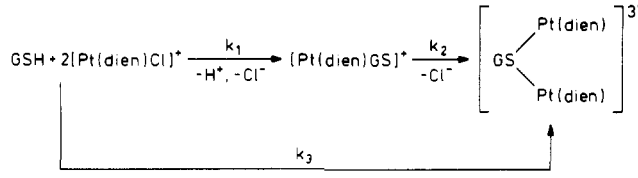

The non-antitumor-active monofunctional [Pt(dien)Cl]Cl complex, with the dien (diethylenetriamine) acting as a non-removable tridentate ligand, has proved to be a very useful model for the first-binding step of platinum antitumor compounds to DNA.[10-12]

† On leave from the University of Svetozar Markovic, Faculty of Science Kragujevac, YU-34000 Kragujevac, Yugoslavia.

(1) Rosenberg, B.; Van Camp, L.; Krigas, T. *Nature* **1965**, *205*, 698.
(2) Johnson, N. P.; Hoeschele, J. D.; Rahn, R. O. *Chem. Biol. Interact.* **1980**, *30*, 151.
(3) Dedon P. C.; Borch, R. F. *Biochem. Pharmacol.* **1987**, *36*, 1955.
(4) Bodenner, D. L.; Dedon, P. C.; Keng, P. C.; Borch, R. F. *Cancer Res.* **1986**, *46*, 2745.
(5) LeRoy, A. F.; Thompson, W. C. *J. Natl. Cancer Inst.* **1989**, *81*, 427.
(6) Repta, A. J.; Long, D. F. In *Cisplatin Current Status and New Developments*; Prestayko, A. W., Crooke, S. T., Carter, S. K., Eds.; Academic Press: New York, 1980; p 285.
(7) Corden, B. J. *Inorg. Chim. Acta* **1987**, *137*, 125.
(8) Andrews, P. A.; Murphy, M. P.; Howell, S. B. *Mol. Pharmacol*, **1986**, *30*, 643.
(9) Otvos, J. D.; Petering, D. H.; Shaw, C. F. *Comments Inorg. Chem.* **1989**, *9*, 1.

0020-1669/91/1330-2648$02.50/0